

Light clusters in hot nuclear matter: calibrating the interaction with heavy-ion collisions

Tiago Custódio¹, Alex Rebillard-Soulié², Rémi Bougault², Diégo Gruyer²,

Francesca Gulminelli², Tuhin Malik¹, Helena Pais¹, and Constança Providência¹

¹*CFisUC, Department of Physics, University of Coimbra, 3004-516 Coimbra, Portugal.*

²*Normandie Univ., ENSICAEN, UNICAEN, CNRS/IN2P3, LPC Caen, F-14000 Caen, France.*

(Dated: July 3, 2024)

We propose a Bayesian inference estimation of in-medium modification of the cluster self-energies from light nuclei multiplicities measured in selected samples of central $^{136,124}\text{Xe}+^{124,112}\text{Sn}$ collisions with the INDRA apparatus. The data are interpreted with a relativistic quasi-particle cluster approach in the mean-field approximation without any prior assumption on the thermal parameters of the model. An excellent reproduction is obtained for H and He isotope multiplicities, and compatible posterior distributions are found for the unknown thermal parameters.

We conclude that the cluster- σ -meson coupling is temperature dependent, becoming weaker when the temperature increases, in agreement with microscopic quantum statistical calculations. This implies a faster decrease of the light cluster abundances with temperature than previously estimated.

Introduction: With the increase of precision on the determination of the static properties and thermal evolution of compact objects by multi-messenger observations, neutron stars can be considered as true laboratories of baryonic matter under extreme conditions. In particular, it is expected that the wider frequency window and larger sensitivity of the next generation of gravitational wave (GW) detectors [1, 2], will allow the detection of supernova and post-merger signals [3–5]. Larger sensitivity and the interpretation of non-modelled GW waveforms with their connection with the electromagnetic counterpart from numerical relativity simulations, require the use of temperature and composition dependent EoS [6], with in particular the inclusion of light cluster formation [7]. Their abundance can indeed affect the dynamics and properties of supernovae [8–10] and binary neutron star mergers [11–15] both directly through their weak reactions with the surrounding medium [16] and indirectly because of their competition with heavy nuclei [17], which can modify the proton fraction and size of the nucleosynthesis seeds [6].

Ab-initio calculations of nuclear clustering in dense media start to be available [18–21], but general purpose EoS used in large scale astrophysical simulations [22] still require the use of mean-field models where light clusters are introduced as independent quasi-particles coupled to effective mesonic fields [7, 17] with couplings calibrated on heavy-ion (HI) experimental data [23, 24]. In the first attempts of optimizing the cluster couplings on HI data [23–25], statistical isothermal samples were tentatively selected by sorting the data in $N_v = 13$ bins of the average radial velocity (v_{surf}) in the expanding source reference frame. The baryonic densities and temperatures associated with the samples were obtained by considering that the statistical ensembles of particles could be described by an ideal gas of classical clusters in the grand canonical ensemble [23–25], while in a more recent work [26, 27] a parameterised correction to ideal Boltzmann

yields was added. In the present study, we propose to analyse the data avoiding the ideal gas assumption, thus providing for the first time hypothesis-independent estimation of the in-medium corrections. The compatibility of the results using independent analyses of four different data sets varying in size and isospin content will a-posteriori prove the statistical character of the samples, and allow estimating the systematical uncertainty within a Bayesian framework.

Data analysis: For this analysis, we use selected INDRA data sets corresponding to the center of mass (CM) emitting source produced with four different entrance channels $^{136,124}\text{Xe}+^{124,112}\text{Sn}$ at 32 MeV/nucleon [28]. Only central events are considered and data are sorted in bins of the average Coulomb-corrected particle velocities v_{surf} in the CM frame [23, 24], that was shown to be correlated to the dynamics of the expansion, and therefore to the effective temperature of the source [23].

The validity of chemical equilibrium in the selected samples was experimentally verified for all Hydrogen and Helium isotopes with the exception of ^6He [29] which suffers from finite-size effects and is therefore excluded from the analysis. The global proton fraction of the samples can be safely deduced from the data with minimal hypotheses on the undetected neutrons [24], but other thermodynamic quantities such as the baryon density ρ and the temperature T are not measured experimentally and must be obtained indirectly from the chemical equilibrium requirement. To this aim, we use a relativistic mean-field formalism, which includes nucleons and light nuclear clusters as independent quasi-particles and takes into account the expected in-medium effects of light clusters in a dense medium [7, 30–32]. The interactions are mediated by the exchange of virtual mesons: the isoscalar-scalar σ -meson, the isoscalar-vector ω -meson and the isovector-vector ρ -meson. The corresponding La-

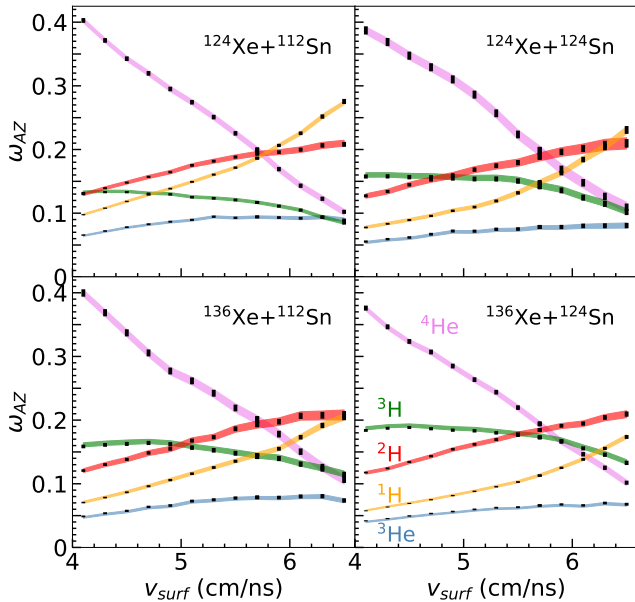


Figure 1: Experimental (black symbols) and theoretical (colour bands) nuclear species mass fractions for the different colliding systems $^{136,124}\text{Xe}+^{124,112}\text{Sn}$ and with the optimised (ρ, T, x_s) parameter distributions displayed in Figs.2,3. All quantities are represented with $2\text{-}\sigma$ uncertainty.

grandian density reads [32, 33]

$$\mathcal{L} = \sum_{\substack{j=n,p, \\ ^2\text{H}, ^3\text{H}, \\ ^3\text{He}, ^4\text{He}}} \mathcal{L}_j + \sum_{m=\sigma,\omega,\rho} \mathcal{L}_m + \mathcal{L}_{\omega\rho}, \quad (1)$$

where the first term describes the nucleons and light clusters interacting with the mesons, the second term describes the meson fields, including self-interacting terms, and the last term is a mixed non-linear meson term, involving the ρ and ω -mesons. The meson-nucleon couplings, denoted by g_{mN} , where $m = \sigma, \omega, \rho$, are fitted to nuclear properties. In the following we present results considering the FSU parameterisation [34], which has been calibrated to the ground state properties of finite nuclei and their linear response, and is therefore suitable to describe low-density matter. The meson-cluster couplings are defined as $g_{\sigma j} = x_s A_j g_{\sigma N}$, $g_{\omega j} = A_j g_{\omega N}$, where A_j is the mass number of cluster and the coupling ratio $x_s(\rho, T)$ measures the (possibly density and temperature dependent) in-medium modification of the cluster self-energies, and is calibrated on the experimental data.

We carry out $4N_v = 52$, one for each system and v_{surf} bin, independent Bayesian inferences on the measured mass fractions $\omega_{AZ} = AY_{AZ}/A_T$ of the different clusters with mass number A and charge Z , where Y_{AZ} are the multiplicities and A_T is the total number of nucleons. Independent posterior distributions of the model

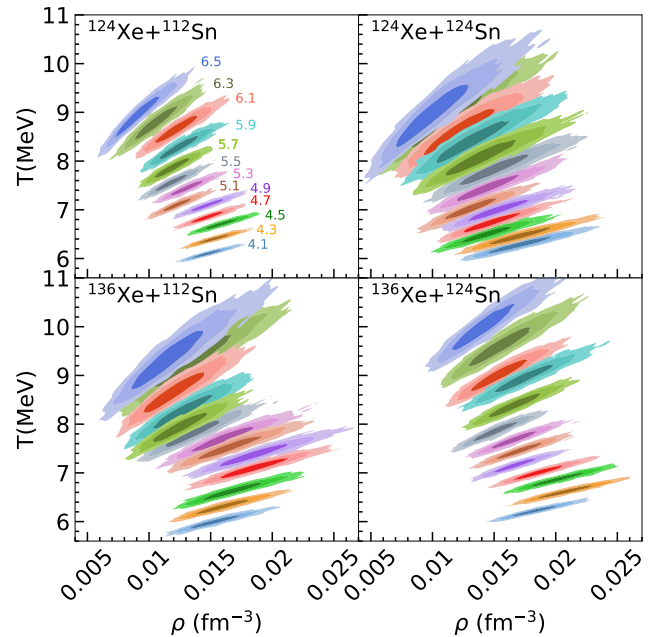


Figure 2: Bayesian estimation of the thermodynamical parameters ρ and T for the different experimental samples. Each colour represents a different v_{surf} (cm/ns) bin and is identified on the upper left panel. For each band, the 1,2,3- σ uncertainty regions are shown.

parameters $\theta = \{T, \rho, x_s(\rho, T)\}$ are obtained for each $i = 1, \dots, 4N_v$ velocity bin and each system, according to:

$$p_i(\theta|\{\omega_{AZ}\}) = \frac{p_\theta}{\mathcal{Z}} \mathcal{L}_g(\{\omega_{AZ}\}_i|\theta), \quad (2)$$

where p_θ is a flat prior, \mathcal{Z} is the evidence, $\{\omega_{AZ}\}_i$ is the i -th mass fraction data set from Ref.[29], and \mathcal{L}_g is a gaussian likelihood [35]. To perform the inference, we have used the PyMultiNest sampler [36, 37], which divides the posterior into nested slices with initial n -live points, generating samples from each and recombining them to restore the original distribution [38].

The quality of the calibration is clearly seen from Fig. 1 where the experimentally measured mass fractions (black symbols) are compared with the corresponding marginalised posteriors obtained integrating Eq.(2) over the (T, ρ, x_s) distributions. This is at variance with the previous analyses [26, 27], where ^2H , ^3H and ^3He abundances are not reproduced, and the experimental ^4He abundances are outside the theoretical predictions for some temperature ranges, while ^1H is reasonably well reproduced (see Fig. 7 of the Supplemental Material). This seems to imply that important information is lost when the equilibrium constants, a derived quantity from the directly measured observables, are used to calibrate the RMF model.

Results and discussion: In the following, the results shown in Fig. 2 are discussed. For all Xe+Sn systems, the extracted temperatures distributions are relatively wide, however, the average values are very close to the simplified ideal gas assumption [39] used in previous analyses [23, 24, 27], see Fig. 6 Supplemental Material. Still, the temperature clearly increases as v_{surf} increases, and a temperature evolution can be inferred from the data like in the previous analyses.

The same does not occur for the baryonic density: although a small density dependence can be identified with a slight decrease of the density when v_{surf} increases, the results are also compatible with a single density, $\sim 0.015 \text{ fm}^{-3}$, due to the wide distributions in the density domain. We identify this density as the chemical freeze-out density at the surface of the emitting source, below which the particles do not feel anymore the nuclear interaction at each step of the cooling process.

This result is at variance with previous analyses [23, 24, 26, 27] where different prescriptions for the expected density were used, but the assumption of an effective density increasing with v_{surf} was always used. The direct extraction of the unknown effective density from the experimental data set via the Bayesian analysis is at the origin of the excellent reproduction of the experimental data in Fig. 1. It might be interesting to observe that the freeze-out picture was already advanced to interpret INDRA vaporization data [40], where multiplicities were very well reproduced with the explicit hypothesis that whatever the effective temperature, fragmentation data bear information on a single density, tentatively identified with the condition of chemical freeze-out.

Taking these results into account, we will interpret the Bayesian results as follows: a) The selected INDRA data only gives information on a single value of the baryonic density, which we will take to be $\approx 0.015 \text{ fm}^{-3}$. We will assume that the ratio x_s does not vary with the baryonic density within the limited range explored by the data; b) The data test temperatures in the range $\sim 6 \text{ MeV}$ to $\sim 10 \text{ MeV}$. There is a temperature dependence of the coupling x_s corresponding to a weakening of the interaction with temperature, i.e. smaller values of x_s correspond to the larger values of temperature.

In Fig. 3 the calibrated values for the x_s are plotted as a function of the temperature, for all v_{surf} values and colliding systems. The decreasing trend of x_s as a function of the temperature is clearly seen for all the four systems. Using the `lmfit` tools [41], we performed a quadratic fitting of x_s with respect to temperature T . The optimal quadratic model, $x_s = aT^2 + bT + c$, was chosen from several possibilities based on fit indices such as χ^2 , Akaike Information Criterion (AIC) and Bayesian Information Criterion (BIC) [42, 43]. Notably, the BIC includes a penalty for models with more parameters. We consider the data of the four colliding systems together, see Table I for the fit parameters along with 1σ and 2σ uncertainty.

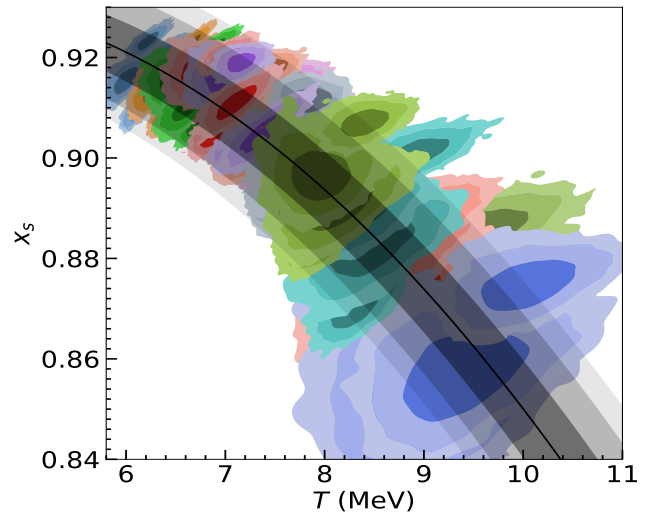


Figure 3: Posterior distributions of the effective cluster coupling parameter x_s as a function of the temperature T . Each colour corresponds to a specific v_{surf} bin as in Fig. 2) and the four distributions per colour correspond to the four independent inferences performed on the different colliding systems. A quadratic fit $x_s = aT^2 + bT + c$ of the global data is represented in black, the median (black solid line) together with the 1,2,3- σ uncertainty regions (the parameters of the fit are shown in Table I).

The decreasing trend of x_s as a function of T is well described by this fit within 3- σ confidence interval.

Table I: Parameter estimates a, b, c with 1, 2σ uncertainties for the model $x_s = aT^2 + bT + c$, as depicted in Figure 3, where T is measured in MeV.

Parameter	Unit	Median	1σ	2σ
a	MeV^{-2}	-0.00203	± 0.00003	± 0.00006
b	MeV^{-1}	0.01477	± 0.00047	± 0.00093
c		0.90560	± 0.0018	± 0.00355

In order to analyse how the temperature dependence of x_s influences the light cluster abundances, in Fig. 4 we compare the total cluster abundances predicted by the RMF FSU model when considering this temperature dependence (red band), and when taking a constant value $x_s = 0.92 \pm 0.02$ as in Refs.[26, 27] (blue band). A total proton fraction of 0.45 was considered as an example within the range of values explored in the four systems [24]. Below $T \lesssim 8 \text{ MeV}$ the two bands overlap, but above this temperature the abundances predicted by the present study are systematically lower than the predictions of [26, 27]. This difference is larger than 20% for $T \sim 10 \text{ MeV}$. Since the σ -meson is responsible for the attractive strong force, a smaller x_s corresponds to a

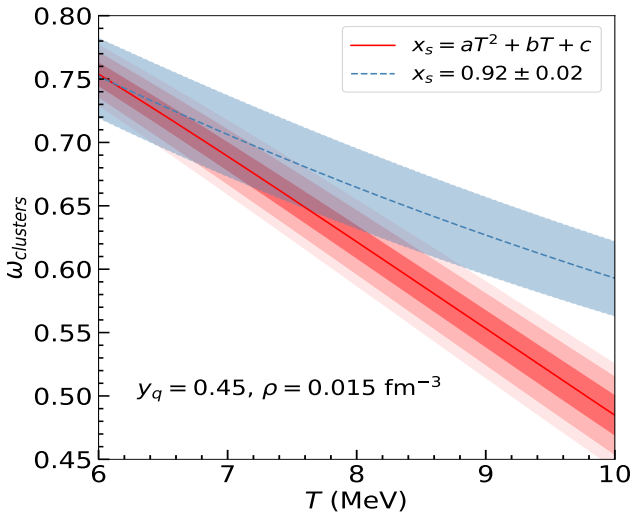


Figure 4: Model (FSU) prediction of the total cluster mass fraction as a function of temperature T with proton fraction $y_q = 0.45$ and baryonic density $\rho = 0.015 \text{ fm}^{-3}$ considering for the σ -cluster coupling ratio x_s the function $x_s(T)$ (solid red) introduced in the present work and a uniform $x_s = 0.92 \pm 0.02$ band from Refs.[26, 27] (dashed blue).

weaker cluster- σ coupling, resulting in less bound clusters and, consequently, smaller abundances.

Conclusions: $^{136,124}\text{Xe} + ^{124,112}\text{Sn}$ central collisions at 32 MeV/nucleon detected with the INDRA apparatus [28], and sorted in bins of the average Coulomb corrected radial velocity v_{surf} , have been studied with an agnostic Bayesian analysis without a-priori hypotheses on the effective temperature and density explored by the different data samples. A Bayesian inference was performed within a RMF description of clusterized matter in order to determine the a-priori density and temperature dependent effective cluster couplings. We limit ourselves to nuclear species for which the samples correspond to chemical equilibrium and finite size effects can be neglected. The validity of the statistical treatment of the samples was a-posteriori verified by the fact that (i) excellent quality fits were obtained for all cluster species whose abundances verify chemical equilibrium [29], (ii) compatible distributions were obtained for the effective coupling ratio $x_s(\rho, T)$ using the four different entrance channels.

The data showed a clear temperature dependence for x_s , but the density resolution was not sufficient to extract a possible density dependence (see also Fig. 5 of Supplemental material). The temperature dependence was parametrized in terms of a quadratic function. The average density extracted from the data analysis, $\sim 0.015 \text{ fm}^{-3}$ was interpreted as a freeze-out density.

It is important to identify the two main differences con-

sidered in the present data analysis with respect to previous ones: (i) instead of calibrating the nuclear model using the equilibrium constants, which are ratios of the measured multiplicities that erase a large part of the entrance channel dependence and the associated information, in the present study the in-medium corrections are calibrated directly using the measured particle abundances; this additionally allows an a-posteriori verification of the equilibrium hypothesis by comparing the different entrance channels; (ii) in the previous analyses, the effective temperature and baryon densities associated to the data samples were estimated from the data within the hypothesis of a grand-canonical ideal gas of classical clusters[23, 24]. Possible effects of the in-medium corrections and quantum effects in the parameter estimation were already considered in [27], but only through a parametrized analytical correction to the ideal gas. In the present analysis, these hypotheses are relaxed and each estimation is performed within an independent Bayesian inference. In this way, the only residual hypotheses concern the nuclear model in itself. For this study, we have used an RMF quasi-particle approach employing the FSU Lagrangian, but it will be important to extend the Bayesian analysis also to the parameters of the nucleonic model in the future.

Compared to previous results, the present study predicts a weaker attractive interaction at higher temperatures and, as a consequence, a faster dissolution of the clusters with temperature. These conclusions are in agreement with microscopic quantum statistical calculations [19]. Our results have clear implications for environments such as a supernova core collapse or a binary neutron star merger, where the presence of clusters affects the transport properties. In the future, it would be very interesting to be able to test different HI reaction mechanisms and entrance channels such as possibly exploring a wider range of temperatures and densities.

ACKNOWLEDGEMENTS

This work was partially supported by the IN2P3 Master Project NewMAC, the ANR project ‘Gravitational waves from hot neutron stars and properties of ultra-dense matter’ (GW-HNS, ANR-22-CE31-0001-01), national funds from FCT (Fundação para a Ciência e a Tecnologia, I.P, Portugal) under projects UIDB/04564/2020 and UIDP/04564/2020, with DOI identifiers 10.54499/UIDB/04564/2020 and 10.54499/UIDP/04564/2020, respectively, and the project 2022.06460.PTDC with the associated DOI identifier 10.54499/2022.06460.PTDC. T.C. acknowledges the grant PRT/BD/154193/2022 (FCT, Portugal). H.P. acknowledges the grant 2022.03966.CEECIND (FCT, Portugal) with DOI identifier 10.54499/2022.03966.CEECIND/CP1714/CT0004.

The authors acknowledge the Laboratory for Advanced Computing at the University of Coimbra for providing HPC resources that have contributed to the research results reported within this paper, URL: <https://www.uc.pt/lca>. We acknowledge support from

Région Normandie under RIN/FIDNEOS and support from Portugal/France PESSOA program (PHC 47833UB France, 2021.09262.CBM Portugal).

Light clusters in hot nuclear matter: calibrating the interaction with heavy-ion collisions Supplemental Material

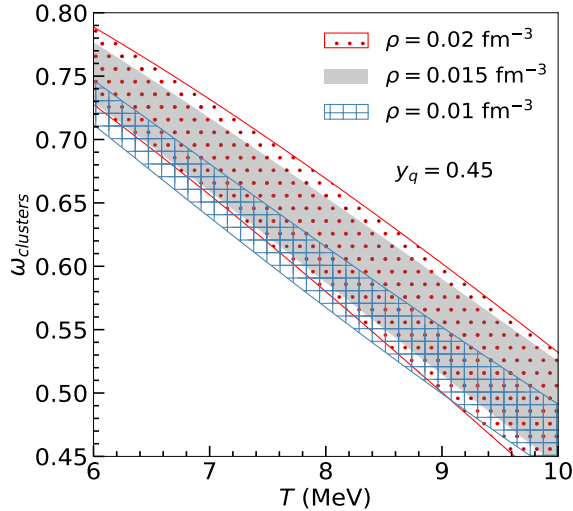


Figure 5: Sum of the mass fractions of ${}^2\text{H}$, ${}^3\text{H}$, ${}^3\text{He}$, ${}^4\text{He}$ ($\omega_{clusters}$) for the FSU RMF model considering the quadratic dependence of x_s with T , obtained for three different baryonic densities, 0.01, 0.015 and 0.02 fm^{-3} , and the proton fraction 0.45. The bands correspond to 3- σ error bands of the quadratic fit.

To check the validity of the assumption that all v_{surf} measurements can be assigned to the same baryonic density, we plot in Fig. 5, for the proton fraction 0.45, the abundance of light clusters for three different values of the baryonic density, 0.01, 0.015 and 0.02 fm^{-3} , which is the range of calibrated values shown in Figure 2 of the main letter. The differences obtained are all within the error bands, supporting our assumption that there is no density dependence on x_s .

In Fig. 6, we show the comparison between the calibrated values of the temperature and baryonic density performed within the Bayesian framework used in the present work (symbols with errorbars) and the ones estimated considering the ideal gas assumption from Ref.[24] (lines). The temperatures in the ideal gas framework were obtained considering the statistical approach of Ref.[39]. In both pictures, the results for the temperature are in agreement. The same does not occur for the baryonic density: in the ideal gas assumption, the density increases as a function of the v_{surf} ; whereas the present

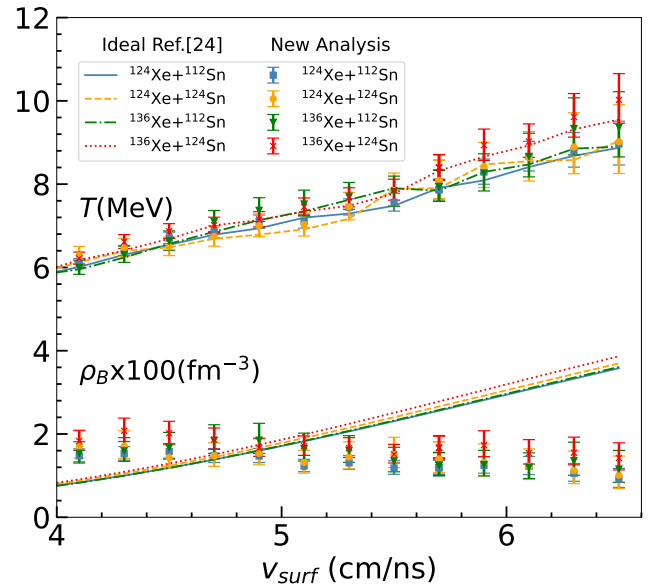


Figure 6: Comparison between the calibrated values of the temperature and baryonic density (symbols with errorbars) performed within the bayesian framework used in the present work and the ones estimated considering the ideal gas assumption from Refs.[24] (lines).

results are compatible with a single density, $\sim 0.015\text{ fm}^{-3}$ that we identify with the chemical freeze-out density, below which the particles do not feel anymore the nuclear interaction.

In Fig. 7, we show the mass fractions experimentally measured in Refs. [24, 29] and analysed considering in-medium effects Refs. [26, 27] as a function of the density, and we compare them with the theoretical ones calculated with the FSU model considering the extracted values of ρ , T and y_p from Refs. [26, 27], together with the x_s coupling that was fitted to the chemical equilibrium constants found in that previous study. We notice that the deuteron, ${}^3\text{H}$ and ${}^3\text{He}$ abundances are not reproduced, and the experimental ${}^4\text{He}$ abundances are outside the theoretical predictions for some temperature ranges, while the proton is reasonably well reproduced.

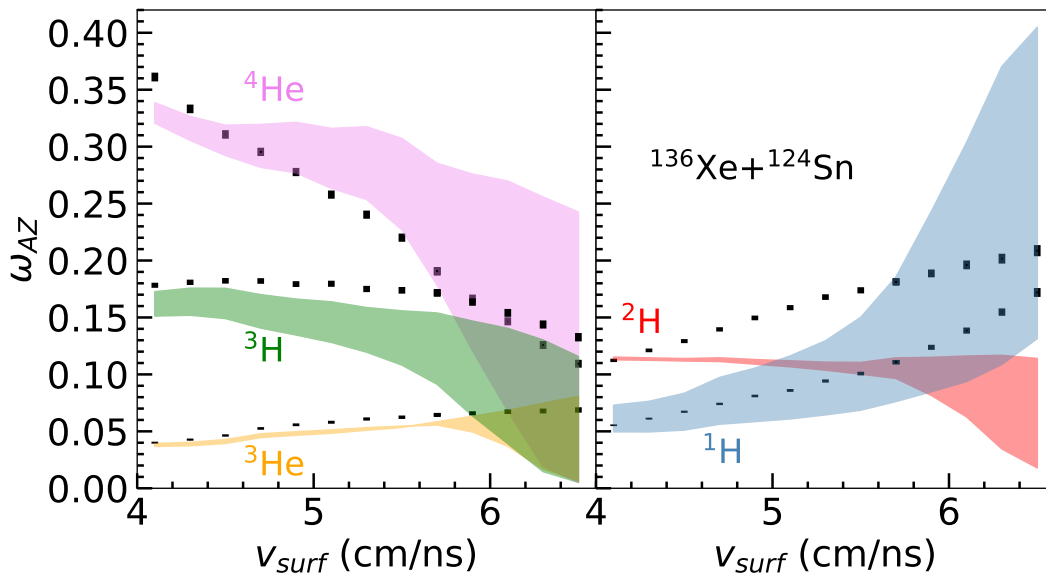


Figure 7: Comparison between experimentally measured mass fractions (black) [24] analysed under the assumptions of [27], and the mass fractions calculated with FSU RMF model using the temperatures, densities, proton fractions and x_s obtained in [26, 27] (colour) for the system $^{136}\text{Xe}+^{124}\text{Sn}$. Note that ^6He was included in the analysis, and, therefore, the experimental data used differ from the one considered in the present study. All quantities are represented with $1\text{-}\sigma$ uncertainty.

-
- [1] M. Branchesi et al., JCAP **07**, 068, arXiv:2303.15923 [gr-qc].
- [2] M. Evans et al., (2021), arXiv:2109.09882 [astro-ph.IM].
- [3] K. Chatziioannou, Phys. Rev. D **105**, 084021 (2022), arXiv:2108.12368 [gr-qc].
- [4] D. Radice, S. Bernuzzi, and A. Perego, Ann. Rev. Nucl. Part. Sci. **70**, 95 (2020), arXiv:2002.03863 [astro-ph.HE].
- [5] Z. Carson, K. Chatziioannou, C.-J. Haster, K. Yagi, and N. Yunes, Phys. Rev. D **99**, 083016 (2019), arXiv:1903.03909 [gr-qc].
- [6] V. Nedora, S. Bernuzzi, D. Radice, B. Daszuta, A. Endrizzi, A. Perego, A. Prakash, M. Safarzadeh, F. Schianchi, and D. Logoteta, The Astrophysical Journal **906**, 98 (2021).
- [7] S. Typel, G. Ropke, T. Klahn, D. Blaschke, and H. H. Wolter, Phys. Rev. C **81**, 015803 (2010), arXiv:0908.2344 [nucl-th].
- [8] A. Arcones, G. Martínez-Pinedo, E. O'Connor, A. Schwenk, H.-T. Janka, C. J. Horowitz, and K. Langanke, Phys. Rev. C **78**, 015806 (2008).
- [9] K. Sumiyoshi and G. Ropke, Phys. Rev. C **77**, 055804 (2008), arXiv:0801.0110 [astro-ph].
- [10] S. Furusawa, H. Nagakura, K. Sumiyoshi, and S. Yamada, Astrophys. J. **774**, 78 (2013), arXiv:1305.1510 [astro-ph.HE].
- [11] A. Bauswein, S. Goriely, and H. T. Janka, Astrophys. J. **773**, 78 (2013), arXiv:1302.6530 [astro-ph.SR].
- [12] S. Rosswog, Int. J. Mod. Phys. D **24**, 1530012 (2015), arXiv:1501.02081 [astro-ph.HE].
- [13] D. Radice, A. Perego, K. Hotokezaka, S. A. Fromm, S. Bernuzzi, and L. F. Roberts, Astrophys. J. **869**, 130 (2018), arXiv:1809.11161 [astro-ph.HE].
- [14] G. Navó, M. Reichert, M. Obergaulinger, and A. Arcones, Astrophys. J. **951**, 112 (2023), arXiv:2210.11848 [astro-ph.HE].
- [15] A. Psaltis, M. Jacobi, F. Montes, A. Arcones, C. J. Hansen, and H. Schatz, Astrophys. J. **966**, 11 (2024), arXiv:2312.12306 [astro-ph.HE].
- [16] T. Fischer, S. Typel, G. Röpke, N.-U. F. Bastian, and G. Martínez-Pinedo, Phys. Rev. C **102**, 055807 (2020).
- [17] H. Pais, F. Gulminelli, C. Providência, and G. Röpke, Phys. Rev. C **99**, 055806 (2019).
- [18] G. Ropke, Nucl. Phys. A **867**, 66 (2011), arXiv:1101.4685 [nucl-th].
- [19] G. Röpke, Phys. Rev. C **92**, 054001 (2015), arXiv:1411.4593 [nucl-th].
- [20] G. Röpke, Phys. Rev. C **101**, 064310 (2020).
- [21] Z. Ren, S. Elhatisari, T. A. Lähde, D. Lee, and U.-G. Meißner, Physics Letters B **850**, 138463 (2024).
- [22] S. Typel, M. Oertel, and T. Klähn, Phys. Part. Nucl. **46**, 633 (2015), arXiv:1307.5715 [astro-ph.SR].
- [23] L. Qin et al., Phys. Rev. Lett. **108**, 172701 (2012), arXiv:1110.3345 [nucl-ex].
- [24] R. Bougault et al., J. Phys. G **47**, 025103 (2020), arXiv:1911.08355 [nucl-ex].
- [25] M. Hempel, K. Hagel, J. Natowitz, G. Röpke, and S. Typel, Phys. Rev. C **91**, 045805 (2015), arXiv:1503.00518 [nucl-th].
- [26] H. Pais et al., J. Phys. G **47**, 105204 (2020), arXiv:2006.07256 [nucl-th].
- [27] H. Pais et al., Phys. Rev. Lett. **125**, 012701 (2020).
- [28] R. Bougault et al. (INDRA Collaboration), Phys. Rev. C **97**, 024612 (2018).

- [29] A. Rebillard-Soulié *et al.*, *Journal of Physics G: Nuclear and Particle Physics* **51**, 015104 (2023).
- [30] M. Ferreira and C. Providencia, *Phys. Rev. C* **85**, 055811 (2012), arXiv:1206.0139 [nucl-th].
- [31] H. Pais, S. Chiacchiera, and C. Providência, *Phys. Rev. C* **91**, 055801 (2015), arXiv:1504.03964 [nucl-th].
- [32] H. Pais, F. Gulminelli, C. Providência, and G. Röpke, *Phys. Rev. C* **97**, 045805 (2018).
- [33] T. Custódio, H. Pais, and C. Providência, *Phys. Rev. C* **104**, 035801 (2021).
- [34] B. G. Todd-Rutel and J. Piekarewicz, *Phys. Rev. Lett.* **95**, 122501 (2005), arXiv:nucl-th/0504034.
- [35] A. Gelman, J. B. Carlin, H. S. Stern, D. B. Dunson, A. Vehtari, and D. B. Rubin, *Bayesian Data Analysis*, 3rd ed. (CRC Press, 2013).
- [36] J. Buchner, A. Georgakakis, K. Nandra, L. Hsu, C. Rangel, M. Brightman, A. Merloni, M. Salvato, J. Donley, and D. Kocevski, *Astron. Astrophys.* **564**, A125 (2014), arXiv:1402.0004 [astro-ph.HE].
- [37] J. Buchner 10.1214/23-ss144 (2021), arXiv:2101.09675 [stat.CO].
- [38] J. Skilling, *AIP Conference Proceedings* **735**, 395 (2004), <https://aip.scitation.org/doi/pdf/10.1063/1.1835238>.
- [39] S. Albergo *et al.*, *Il Nuovo Cimento A* **89** (1985).
- [40] B. Borderie *et al.*, *Physics Letters B* **388**, 224 (1996).
- [41] M. Newville, T. Stensitzki, D. B. Allen, and A. Ingargiola, *lmfit: Non-linear least-squares minimization and curve-fitting for python* (2020), accessed: [7 May 2024].
- [42] H. Akaike, *IEEE Transactions on Automatic Control* **19**, 716 (1974).
- [43] G. Schwarz, *The Annals of Statistics* **6**, 461 (1978).